FAILURE ANALYSIS OF A CFRP RUN-OUT CONFIGURATION WITH BUTT-STRAP JOINT

A. Estefani[a], A. Blázquez[a*], J. Reinoso[b], F. París[a], J. Cañas[a]

[a]*Grupo de Elasticidad y Resistencia de Materiales, ETS de Ingeniería, Universidad de Sevilla*
[b] *Institut für Statik und Dynamik, Leibniz Universität Hannover, Germany*
**abg@etsi.us.es*

Keywords: Design, Damage Mechanics, Mechanical testing, FEM.

Abstract
In a stiffened panel, run-out regions are areas where the stiffener is interrupted. The load path is changed substantially around these areas, which are identified as critical regions of the structure. This paper deals with the numerical and experimental analyses of a specimen that simulates the local geometry of a run-out region near a frame of an aircraft fuselage. In the case investigated here, a run-out conception including a butt-strap is used to alleviate the abrupt load transfer between adjacent sections; with and without stiffener.

1. Introduction

There have been many structural systems conceived over the years to support the load acting on an aircraft. The established convention for the structure of an aircraft fuselage or wing consists of an arrangement of some members in transversal direction (called ribs in the wings and frames or rings in the fuselage) and another members in longitudinal direction (called stringers). Nevertheless, this structural typology is not exclusive of aircraft and it is used widely in engineering because of its high efficiency.

The design of the points where the stringers cross the frames (or the ribs) is not easy. Many different arrangements are used (see [1]), most of them requiring auxiliary devices and the corresponding rivets to ensure the correct joint of the whole system. Some of these designs imply a cut-out of the frame (to allow the stringer to pass through it) while others require the interruption of the stringers. On the one hand, a cut-out of the frame introduces unavoidable stress concentrations which should be minimized. On the other hand, the interruption of the stringers makes compulsory the use of clips which have to be carefully designed.

Nowadays, composite materials are being incorporated in the manufacturing of aircraft structures, increasing their efficiency due to the high specific strength and stiffness of these materials. Although behavior and, which is more significant, failure of composite material are very different of metal, the aforementioned joints for composite materials are usually designed using the same solutions than for metal.

The work presented here is a part of an extensive program that analyzed, experimental and numerically, the behavior and damage tolerance of several design concepts for the crossing point of the stringer and the frame in a fuselage panel, [2][3]. For all the designs considered,

the stringers were interrupted at some distance from the frame, in this way clips and other devices for the joint could be avoided, but a run-out region appear. At these areas, a substantial modification of the load transfer path takes place, which made them critical locations of the structure [4].

The specimen under study was monotonically loaded in tension up to collapse. Strain gages, displacement transducers and a load cell were used to monitor the test which was carried out on a universal testing machine Instron-8806. Numerical simulation was performed using the Submodeling global-local technique implemented in ABAQUS® v6.8 [5]; cohesive elements were used to model debonding processes; contact between the parts of the model was considered; finally, fastener tools were applied to simulate the rivets.

2. Specimen description

Figure 1 shows the sketch of the specimen under study in this work. It consisted of a flat skin (300 mm in width at the area of interest), a Ω stringer, a butt-strap, a couple of clips and a dummy frame. Skin, stringers, butt-strap and clips were made of IMA/M21E carbon fiber composite, whereas aluminum alloy 2024-T42 was used for the frame. The panel was manufactured using co-bonded technique, a layer (0.2 mm in thickness) of IMA/M21E resin being used as adhesive (between stringer and skin and between butt-strap and skin).

Laminate sequences at the test area were: $(45/-45/0/0/90/0/0)_S$ for the stringer, $(45/-45/90/0/-45/45/90/90)_\$$ for the skin, $(45/-45/90/0/-45/45/90/0)_S$ for the butt-strap, and $(45/-45/0/0/90/0/0)_S$ for the clips. See reference [2] for material mechanical properties. Four steel rivets were used to fasten each clip with the rest of the component (2 rivets for skin and stringer flange, and another 2 rivets for skin and butt-strap). The ends of the specimen were reinforced to prevent undesirable breakages.

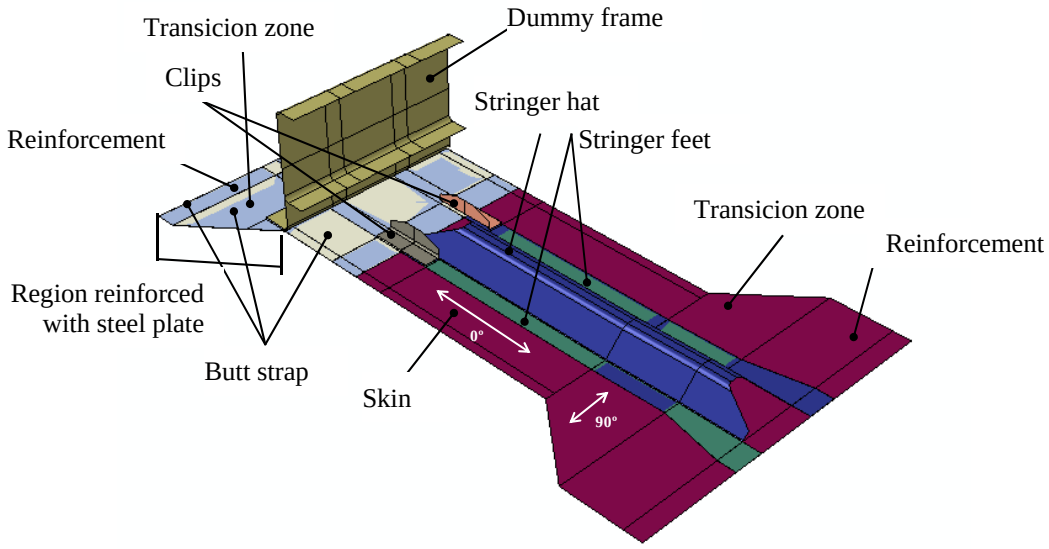

Figure 1. Components of the specimen.

3. Experimental test

A tensile test along the longitudinal direction (0º in Figure 1) was carried out until collapse.

The experimental set-up aimed to reproduce the boundary conditions at the corresponding area of a full scale fuselage, see Figure 2a. The longitudinal ends of the specimen were fastened (three rows of 12 rivets each one) to specifically designed grips; lateral edges were guided (displacement perpendicular to the skin was constrained); finally the top flange of the frame was not allowed to move, neither perpendicularly to the panel nor rotate.

A set of 10 pairs back-to-back longitudinal strain gages was used to record the behavior of the specimen. Figure 2b shows their notation and location. Several visual and ultrasonic inspections were performed during the test in order to identify the onset and development of debonding and/or delamination in the specimen.

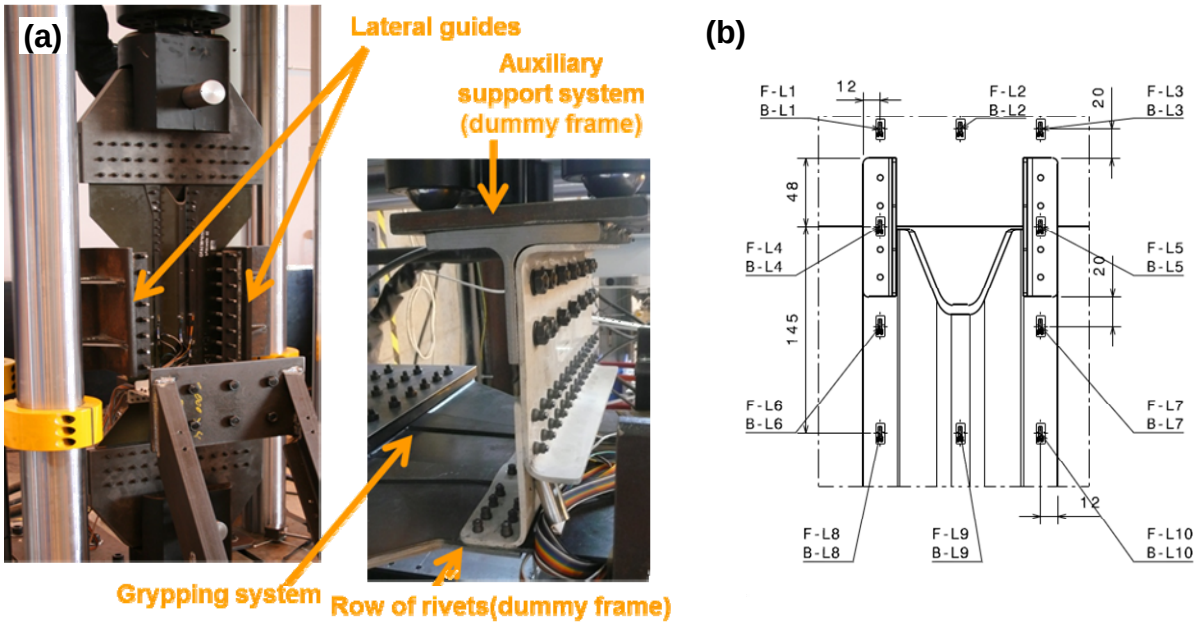

Figure 2. Test details: (a) experimental setup and (b) strain gages notation and location (F=front, B=back).

First audible noise (identified as damage onset) was detected for 64.6 kN. It started at the end of the right stringer flange (see Figure 3). Collapse occurred for 398 kN and was characterized by general debonding between the skin and the stringer and between the skin and the butt-strap. Figure 3 shows a picture of the run-out region after the test.

Figure 3. Detail of the damaged zone around the roun-out region after the test.

4. Finite element model

A finite element model was developed to understand and determine the causes of the events occurring during the test. Due to the geometrical characteristics of the specimen under study, a shell-like model would be the most efficient approach computationally. However, the complex stress states present around the run-out region require the accurate estimation of the full set of stress components, specifically the transverse stress components (neglected by conventional shell models), which are responsible of delamination and debonding events. Thus, solid-based models were selected.

The main difficulty in the use of solid elements is the computational cost, due to the high number of elements required. One possible modeling alternative that furnishes a compromise between numerical efficiency and mechanical accuracy is the global-local *Submodeling* approach implemented in Abaqus® [5]. With this technique the process can be seen as a two-step procedure: (1) a shell-like global model is solved first, and (2) its results are used to define the kinematic conditions for a subsequent detailed solid-like local model. Through this strategy, solid elements were only used for the zone we were interested in. Notice that global conditions affect the local model but results from the local model do not have any influence on the global one.

4.1. Global model

A combination of shell and solid elements was employed for the global model: a thin (in fact it was 0.2 mm) layer of solid elements were used to model the adhesive layer, but shells were used to model the skin, the stringer, the butt-strap, the frame and the clips. In this way, a complete numerical prediction of the full stress tensor was obtained around the adhesive layer, and a size for the local model could be suggested.

Figure 4 shows a scheme of the modeling approach used for the adhesive joint between the skin and the flange of the stringer (analogously for the butt-strap) and a detail of the global mesh. C3D8R elements (linear) were used for the adhesive layer (3400 for the stringer-skin joints and 12150 for the butt-strap-skin joint) and S4R elements (linear) were used for the skin (30850), stringer (10960), butt-strap (12150), clips (2×360) and frame (6160) [5]. Reference surfaces for the skin and for the stringer flange (butt-strap) were defined at the interface with the adhesive layer, in this way the tie between the corresponding surfaces were facilitated. Surfaces of the clips were tied with the corresponding surfaces of the stringer flange or butt-strap.

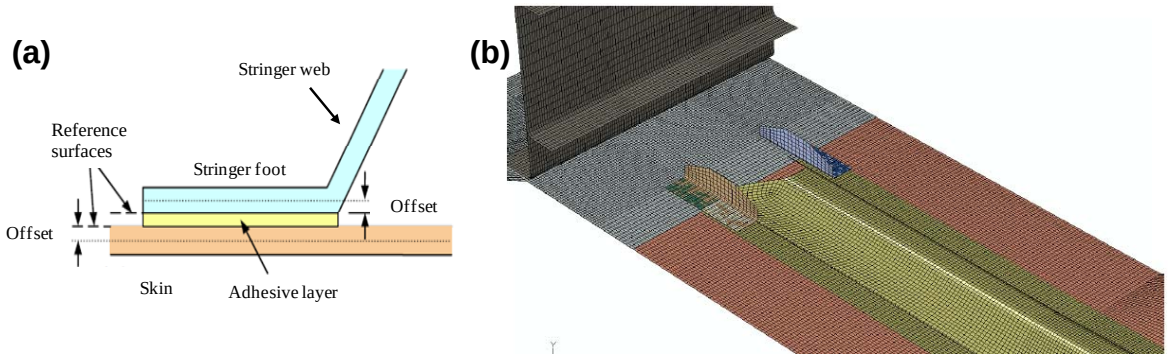

Figure 4. Global model: (a) Shell-solid-shell modelization, and (b) detail of the mesh.

4.2. Local model

The size of the local model was defined taking into account the stress fields around the adhesive layer obtained by the global model (these global results have not been depicted here for conciseness, see [2]). Figure 5a shows the geometrical dimensions of the local model. With respect to the longitudinal plane, the problem was quasi-symmetric (notice that laminates contain $+45^o$ and -45^o plies, which are non-symmetric), and only one of the flanges of the stringers was considered for the local model.

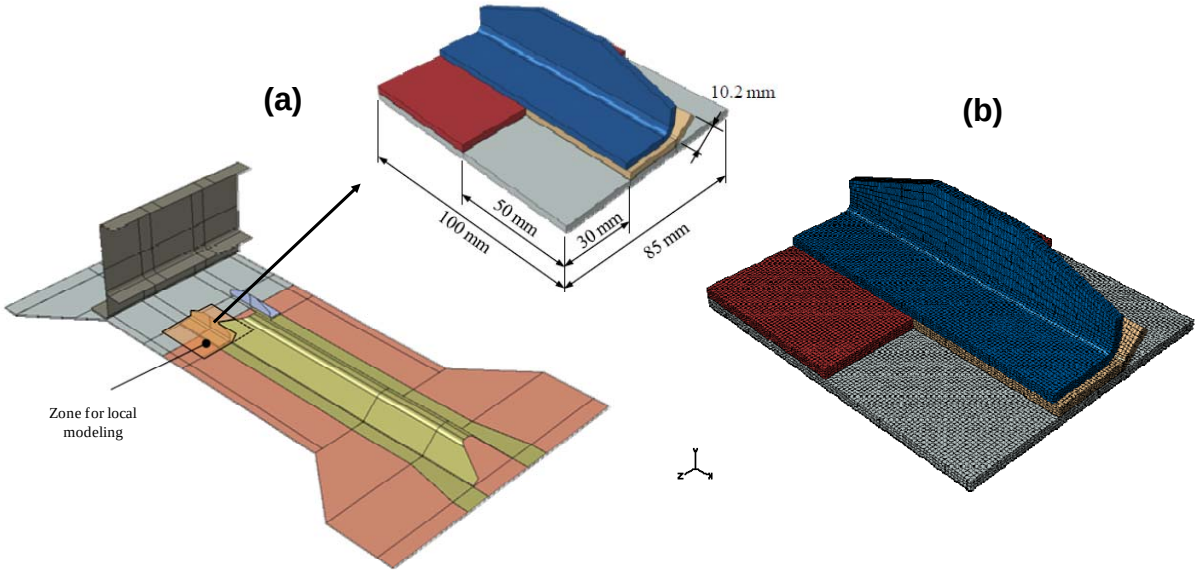

Figure 5. Local model: (a) location in the global model and size, and (b) mesh.

C3D20R elements (parabolic) were used to model entities involved in the local model: portions of skin (25500 elements), stringer (7200 elements), butt-strap (17000 elements) and clip (13068 elements). In order to model the onset and progression of the damage, COH3D8 cohesive elements were used for the adhesive layer (20000 elements for the stringer-skin joint and 68000 for the butt-strap-skin joint) [5]. It has to be mentioned that adhesive mesh and skin, stringer or butt-strap meshes were not conforming each other, adhesive elements being smaller (16 adhesive elements for 1 element of the skin, stringer or butt-strap) than shell elements.

A linear traction-separation law (0.2 mm thickness) was used for the cohesive element. The mechanical characteristics referring to strength, stiffness and toughness were [2]: $E_n = 1477$ Mpa, $G_t = 568$ Mpa, $\sigma_{Ic} = 25.1$ Mpa, $\tau_{IIc} = \tau_{IIIc} = 50$ Mpa, $G_{IC} = 300$ J/m^2, $G_{IIC} = G_{IIIC} = 800$ J/m^2. The maximum normal stress was considered as damage onset criterion, whereas the Benzeggagh and Keane Fracture Criterion (with $\eta = 2.2842$ [6]) extended to three dimensional cases was selected for the mixing failure.

Notice that cohesive elements were included in the local model, but not in the global one. So that damage was only modeled at the local level and boundary conditions transferred from the global model were only valid if the damage zone was small enough that global results will not be potentially affected. In this way, if the size of the damage areas were relatively large, the

onset and initial evolution of the damage could be properly described, but the prediction of the model could be unsatisfactory.

5. Results

First of all, Figure 6 shows the evolution of the measurement of some strain gages (see Figure 2). Experimental results are compared with the numerical evolution computed for the global model. Satisfactory agreement is obtained until 100 kN (remember that no damage is simulated in this model), although in some cases (see plots corresponding to 8 and 10 gages) agreement could be extended until 300 kN (notice that 8 and 10 gages were further from the damage zone than 6 and 7 gages). This fact corroborates the use of the global solutions as boundary conditions for the local model for this load range. Strain evolutions changed suddenly at 300 kN, indicating the damage progressed until the regions around gages locations.

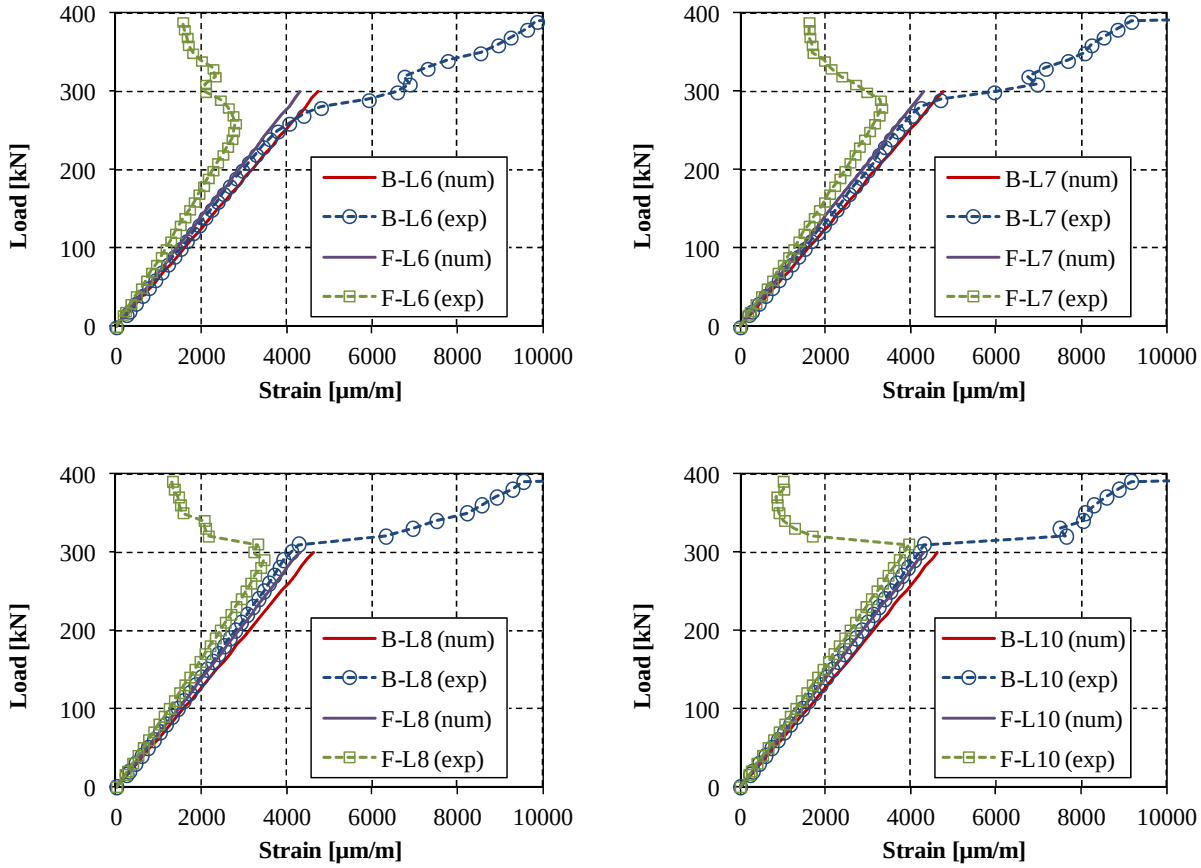

Figure 6. Experimental (exp) and global model numerical (num) results for some strain gages.

Concerning the local analysis, computation run without including any kind of artificial stabilization features. Numerical solution process finished due to convergence difficulties at 113 kN. This load is approximately in the range where global solution agrees with experimental measurements.

Results for the local model are presented in Figures 7 and 8. Figure 7 shows the damage parameter [5] (0 = undamaged, 1 = completely decohesion) for four load levels: 50, 80, 95

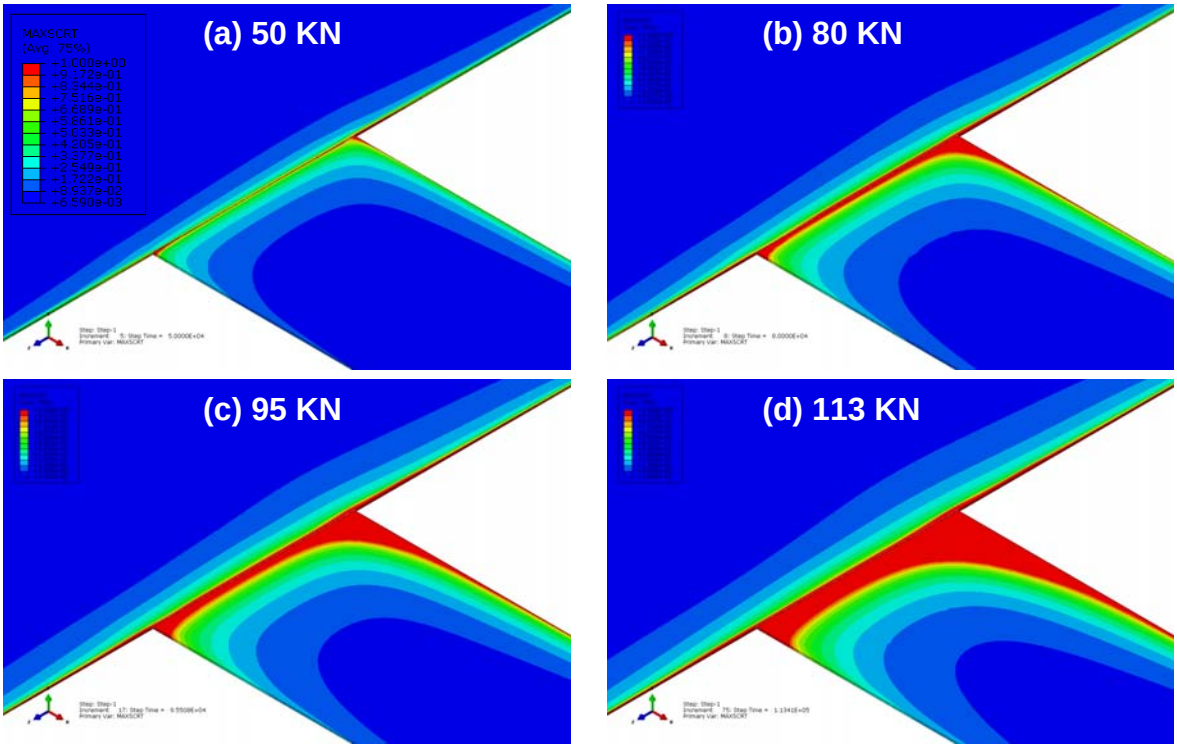

Figure 7. Results for the local model. Damage parameter for (a) 50 kN, (b) 80 kN, (c) 95 kN, and (d) 113 kN.

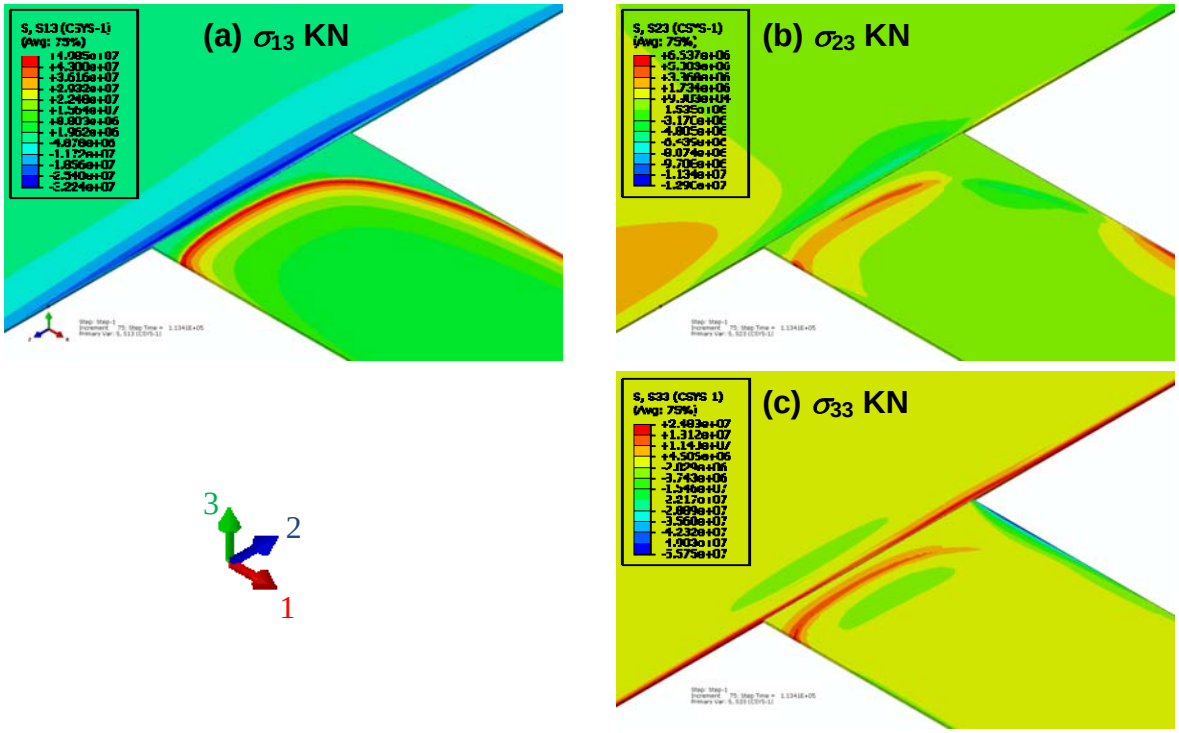

Figure 8. Results for the local model. Transverse stress components for 113 kN.

and 113 kN. Debonding started at the corners of the stringer flange (specifically at the inner one) at around 50 kN, and rapidly evolve along the width of the flange. At 80 kN an additional debonded area was estimated to appear along the edge of the butt-strap. Damage

areas under stringer flange were predicted to progress quickly along the internal boundary of the flange, while damage under the butt-strap increased very slowly. For 113 kN, dimensions of the damaged areas under the stringer foot were about 3 mm width, 15 mm in length along the inner boundary.

Figure 8 shows the transverse stress fields corresponding to 113 kN. In these plots, the extension of the debonding crack under the stringer flange can be clearly appreciated. The crack progressed under mixed mode conditions

6. Conclusions

The stress fields promoted by a specific configuration of the run-out of a stringer near a frame have been analyzed from experimental and numerical points of view. Specimen was loaded in tension until collapse, which occurred at 398 kN. Numerical analysis was performed using a global-local approach, in which the boundary conditions for the refined local model were obtained from the results of a global model. Prior to define the local model, global results were correlated with the experimental measurements. From these results, the size (location was obvious) of the local model was defined. Damage was considered only at the local level, cohesive elements being used for the adhesive layer. From the local model results, damage was predicted to initiate for a load about 50 kN, which approximately coincides with the experimental test load when the first audible sound was detected. The numerical prediction for the initial damaged areas shape agrees with the experimental observation, in which an extensive area of debonding was appreciated under the stringer flange, the damage area under the butt-strap being undetectable. Numerical solution finished at 113 kN due to convergence problems in achieving equilibrium solutions.

Acknowledgements

This research is supported by the Ministerio de Economía y Competitividad of Spain (Project DPI2012-37187) and the Consejería de Economía, Innovación y Ciencia of Junta de Andalucía (Project TEP2011-07093).

References

[1] J. Cutler. *Understanding Aircraft Structures*. Blackwell Pub, 2005.
[2] J. Reinoso, A. Blázquez, A. Estefani, F. París, J. Cañas, E. Arévalo and F. Cruz. Experimental and three-dimensional global-local finite element analysis of a composite component including degradation process at the interfaces. *Composites: Part B*, volume 43:1929-1942, 2012.
[3] J. Reinoso, A. Blázquez, A. Estefani, F. París and J. Cañas. A composite runout specimen subjected to tension-compression loading conditions: experimental and global-local finite element analysis. *Compos. Struct.*, volume 101:274-289, 2013.
[4] S. Psarras, S.T. Pinho, B.G. Falzon. Investigating the use of compliant webs in the damage-tolerant design of stiffener run-outs. *Composites Part B Engineering*, volume 45:70-77, 2013.
[5] *ABAQUS Documentation*. Dassault Systèmes, Providence, RI, USA, 2012.
[6] CG. Dávila, PP. Camanho and A. Turón. Cohesive elements for shells. NASA/TP-2007-214869; 2007.